

Pion-Kaon correlations in Au+Au collisions at $\sqrt{s_{NN}} = 130$ GeV

J. Adams,³ C. Adler,¹² M.M. Aggarwal,²⁵ Z. Ahammed,²⁸ J. Amonett,¹⁷ B.D. Anderson,¹⁷ M. Anderson,⁵ D. Arkhipkin,¹¹ G.S. Averichev,¹⁰ S.K. Badyal,¹⁶ J. Balewski,¹³ O. Barannikova,^{28,10} L.S. Barnby,¹⁷ J. Baudot,¹⁵ S. Bekele,²⁴ V.V. Belaga,¹⁰ R. Bellwied,⁴¹ J. Berger,¹² B.I. Bezverkhny,⁴³ S. Bhardwaj,²⁹ P. Bhaskar,³⁸ A.K. Bhati,²⁵ H. Bichsel,⁴⁰ A. Billmeier,⁴¹ L.C. Bland,² C.O. Blyth,³ B.E. Bonner,³⁰ M. Botje,²³ A. Boucham,³⁴ A. Brandin,²¹ A. Bravar,² R.V. Cadman,¹ X.Z. Cai,³³ H. Caines,⁴³ M. Calderón de la Barca Sánchez,² J. Carroll,¹⁸ J. Castillo,¹⁸ M. Castro,⁴¹ D. Cebra,⁵ P. Chaloupka,⁹ S. Chattopadhyay,³⁸ H.F. Chen,³² Y. Chen,⁶ S.P. Chernenko,¹⁰ M. Cherney,⁸ A. Chikanian,⁴³ B. Choi,³⁶ W. Christie,² J.P. Coffin,¹⁵ T.M. Cormier,⁴¹ J.G. Cramer,⁴⁰ H.J. Crawford,⁴ D. Das,³⁸ S. Das,³⁸ A.A. Derevschikov,²⁷ L. Didenko,² T. Dietel,¹² X. Dong,^{32,18} J.E. Draper,⁵ F. Du,⁴³ A.K. Dubey,¹⁴ V.B. Dunin,¹⁰ J.C. Dunlop,² M.R. Dutta Majumdar,³⁸ V. Eckardt,¹⁹ L.G. Efimov,¹⁰ V. Emelianov,²¹ J. Engelage,⁴ G. Eppley,³⁰ B. Erazmus,³⁴ P. Fachini,² V. Faine,² J. Faivre,¹⁵ R. Fatemi,¹³ K. Filimonov,¹⁸ P. Filip,⁹ E. Finch,⁴³ Y. Fisyak,² D. Flierl,¹² K.J. Foley,² J. Fu,⁴² C.A. Gagliardi,³⁵ M.S. Ganti,³⁸ T.D. Gutierrez,⁵ N. Gagunashvili,¹⁰ J. Gans,⁴³ L. Gaudichet,³⁴ M. Germain,¹⁵ F. Geurts,³⁰ V. Ghazikhanian,⁶ P. Ghosh,³⁸ J.E. Gonzalez,⁶ O. Grachov,⁴¹ V. Grigoriev,²¹ S. Gronstal,⁸ D. Grosnick,³⁷ M. Guedon,¹⁵ S.M. Guertin,⁶ A. Gupta,¹⁶ E. Gushin,²¹ T.J. Hallman,² D. Hardtke,¹⁸ J.W. Harris,⁴³ M. Heinz,⁴³ T.W. Henry,³⁵ S. Heppelmann,²⁶ T. Herston,²⁸ B. Hippolyte,⁴³ A. Hirsch,²⁸ E. Hjort,¹⁸ G.W. Hoffmann,³⁶ M. Horsley,⁴³ H.Z. Huang,⁶ S.L. Huang,³² T.J. Humanic,²⁴ G. Igo,⁶ A. Ishihara,³⁶ P. Jacobs,¹⁸ W.W. Jacobs,¹³ M. Janik,³⁹ I. Johnson,¹⁸ P.G. Jones,³ E.G. Judd,⁴ S. Kabana,⁴³ M. Kaneta,¹⁸ M. Kaplan,⁷ D. Keane,¹⁷ J. Kiryluk,⁶ A. Kisiel,³⁹ J. Klay,¹⁸ S.R. Klein,¹⁸ A. Klyachko,¹³ D.D. Koetke,³⁷ T. Kollegger,¹² A.S. Konstantinov,²⁷ M. Kopytine,¹⁷ L. Kotchenda,²¹ A.D. Kovalenko,¹⁰ M. Kramer,²² P. Kravtsov,²¹ K. Krueger,¹ C. Kuhn,¹⁵ A.I. Kulikov,¹⁰ A. Kumar,²⁵ G.J. Kunde,⁴³ C.L. Kunz,⁷ R.Kh. Kutuev,¹¹ A.A. Kuznetsov,¹⁰ M.A.C. Lamont,³ J.M. Landgraf,² S. Lange,¹² C.P. Lansdell,³⁶ B. Lasiuk,⁴³ F. Laue,² J. Lauret,² A. Lebedev,² R. Lednický,¹⁰ V.M. Leontiev,²⁷ M.J. LeVine,² C. Li,³² Q. Li,⁴¹ S.J. Lindenbaum,²² M.A. Lisa,²⁴ F. Liu,⁴² L. Liu,⁴² Z. Liu,⁴² Q.J. Liu,⁴⁰ T. Ljubicic,² W.J. Llope,³⁰ H. Long,⁶ R.S. Longacre,² M. Lopez-Noriega,²⁴ W.A. Love,² T. Ludlam,² D. Lynn,² J. Ma,⁶ Y.G. Ma,³³ D. Magestro,²⁴ S. Mahajan,¹⁶ L.K. Mangotra,¹⁶ D.P. Mahapatra,¹⁴ R. Majka,⁴³ R. Manweiler,³⁷ S. Margetis,¹⁷ C. Markert,⁴³ L. Martin,³⁴ J. Marx,¹⁸ H.S. Matis,¹⁸ Yu.A. Matulenko,²⁷ T.S. McShane,⁸ F. Meissner,¹⁸ Yu. Melnick,²⁷ A. Meschanin,²⁷ M. Messer,² M.L. Miller,⁴³ Z. Milosevich,⁷ N.G. Minaev,²⁷ C. Mironov,¹⁷ D. Mishra,¹⁴ J. Mitchell,³⁰ B. Mohanty,³⁸ L. Molnar,²⁸ C.F. Moore,³⁶ M.J. Mora-Corral,¹⁹ V. Morozov,¹⁸ M.M. de Moura,⁴¹ M.G. Munhoz,³¹ B.K. Nandi,³⁸ S.K. Nayak,¹⁶ T.K. Nayak,³⁸ J.M. Nelson,³ P. Nevski,² V.A. Nikitin,¹¹ L.V. Nogach,²⁷ B. Norman,¹⁷ S.B. Nurushev,²⁷ G. Odyniec,¹⁸ A. Ogawa,² V. Okorokov,²¹ M. Oldenburg,¹⁸ D. Olson,¹⁸ G. Paic,²⁴ S.U. Pandey,⁴¹ S.K. Pal,³⁸ Y. Panebratsev,¹⁰ S.Y. Panitkin,² A.I. Pavlinov,⁴¹ T. Pawlak,³⁹ V. Perevoztchikov,² W. Peryt,³⁹ V.A. Petrov,¹¹ S.C. Phatak,¹⁴ R. Picha,⁵ M. Planinic,⁴⁴ J. Pluta,³⁹ N. Porile,²⁸ J. Porter,² A.M. Poskanzer,¹⁸ M. Potekhin,² E. Potrebenikova,¹⁰ B.V.K.S. Potukuchi,¹⁶ D. Prindle,⁴⁰ C. Pruneau,⁴¹ J. Putschke,¹⁹ G. Rai,¹⁸ G. Rakness,¹³ R. Raniwala,²⁹ S. Raniwala,²⁹ O. Ravel,³⁴ R.L. Ray,³⁶ S.V. Razin,^{10,13} D. Reichhold,²⁸ J.G. Reid,⁴⁰ G. Renault,³⁴ F. Retiere,¹⁸ A. Ridiger,²¹ H.G. Ritter,¹⁸ J.B. Roberts,³⁰ O.V. Rogachevski,¹⁰ J.L. Romero,⁵ A. Rose,⁴¹ C. Roy,³⁴ L.J. Ruan,^{32,2} V. Rykov,⁴¹ R. Sahoo,¹⁴ I. Sakrejda,¹⁸ S. Salur,⁴³ J. Sandweiss,⁴³ I. Savin,¹¹ J. Schambach,³⁶ R.P. Scharenberg,²⁸ N. Schmitz,¹⁹ L.S. Schroeder,¹⁸ K. Schweda,¹⁸ J. Seger,⁸ D. Seliverstov,²¹ P. Seyboth,¹⁹ E. Shahaliev,¹⁰ M. Shao,³² M. Sharma,²⁵ K.E. Shestermanov,²⁷ S.S. Shimanskii,¹⁰ R.N. Singaraju,³⁸ F. Simon,¹⁹ G. Skoro,¹⁰ N. Smirnov,⁴³ R. Snellings,²³ G. Sood,²⁵ P. Sorensen,⁶ J. Sowinski,¹³ H.M. Spinka,¹ B. Srivastava,²⁸ S. Stanislaus,³⁷ R. Stock,¹² A. Stolpovsky,⁴¹ M. Strikhanov,²¹ B. Stringfellow,²⁸ C. Struck,¹² A.A.P. Suaide,⁴¹ E. Sugarbaker,²⁴ C. Suire,² M. Šumbera,⁹ B. Surrow,² T.J.M. Symons,¹⁸ A. Szanto de Toledo,³¹ P. Szarwas,³⁹ A. Tai,⁶ J. Takahashi,³¹ A.H. Tang,^{2,23} D. Thein,⁶ J.H. Thomas,¹⁸ V. Tikhomirov,²¹ M. Tokarev,¹⁰ M.B. Tonjes,²⁰ T.A. Trainor,⁴⁰ S. Trentalange,⁶ R.E. Tribble,³⁵ M.D. Trivedi,³⁸ V. Trofimov,²¹ O. Tsai,⁶ T. Ullrich,² D.G. Underwood,¹ G. Van Buren,² A.M. VanderMolen,²⁰ A.N. Vasiliev,²⁷ M. Vasiliev,³⁵ S.E. Vigdor,¹³ Y.P. Viyogi,³⁸ S.A. Voloshin,⁴¹ W. Waggoner,⁸ F. Wang,²⁸ G. Wang,¹⁷ X.L. Wang,³² Z.M. Wang,³² H. Ward,³⁶ J.W. Watson,¹⁷ R. Wells,²⁴ G.D. Westfall,²⁰ C. Whitten Jr.,⁶ H. Wieman,¹⁸ R. Willson,²⁴ S.W. Wissink,¹³ R. Witt,⁴³ J. Wood,⁶ J. Wu,³² N. Xu,¹⁸ Z. Xu,² Z.Z. Xu,³² A.E. Yakutin,²⁷ E. Yamamoto,¹⁸ J. Yang,⁶ P. Yepes,³⁰ V.I. Yurevich,¹⁰ Y.V. Zanevski,¹⁰ I. Zborovský,⁹ H. Zhang,^{43,2} H.Y. Zhang,¹⁷ W.M. Zhang,¹⁷ Z.P. Zhang,³² P.A. Żolnierczuk,¹³ R. Zoukarneev,¹¹ J. Zoukarneeva,¹¹ and A.N. Zubarev¹⁰

(STAR Collaboration),*

- ¹Argonne National Laboratory, Argonne, Illinois 60439
- ²Brookhaven National Laboratory, Upton, New York 11973
- ³University of Birmingham, Birmingham, United Kingdom
- ⁴University of California, Berkeley, California 94720
- ⁵University of California, Davis, California 95616
- ⁶University of California, Los Angeles, California 90095
- ⁷Carnegie Mellon University, Pittsburgh, Pennsylvania 15213
- ⁸Creighton University, Omaha, Nebraska 68178
- ⁹Nuclear Physics Institute AS CR, Řež/Prague, Czech Republic
- ¹⁰Laboratory for High Energy (JINR), Dubna, Russia
- ¹¹Particle Physics Laboratory (JINR), Dubna, Russia
- ¹²University of Frankfurt, Frankfurt, Germany
- ¹³Indiana University, Bloomington, Indiana 47408
- ¹⁴Institute of Physics, Bhubaneswar 751005, India
- ¹⁵Institut de Recherches Subatomiques, Strasbourg, France
- ¹⁶University of Jammu, Jammu 180001, India
- ¹⁷Kent State University, Kent, Ohio 44242
- ¹⁸Lawrence Berkeley National Laboratory, Berkeley, California 94720
- ¹⁹Max-Planck-Institut für Physik, Munich, Germany
- ²⁰Michigan State University, East Lansing, Michigan 48824
- ²¹Moscow Engineering Physics Institute, Moscow Russia
- ²²City College of New York, New York City, New York 10031
- ²³NIKHEF, Amsterdam, The Netherlands
- ²⁴Ohio State University, Columbus, Ohio 43210
- ²⁵Panjab University, Chandigarh 160014, India
- ²⁶Pennsylvania State University, University Park, Pennsylvania 16802
- ²⁷Institute of High Energy Physics, Protvino, Russia
- ²⁸Purdue University, West Lafayette, Indiana 47907
- ²⁹University of Rajasthan, Jaipur 302004, India
- ³⁰Rice University, Houston, Texas 77251
- ³¹Universidade de Sao Paulo, Sao Paulo, Brazil
- ³²University of Science & Technology of China, Anhui 230027, China
- ³³Shanghai Institute of Nuclear Research, Shanghai 201800, P.R. China
- ³⁴SUBATECH, Nantes, France
- ³⁵Texas A & M, College Station, Texas 77843
- ³⁶University of Texas, Austin, Texas 78712
- ³⁷Valparaiso University, Valparaiso, Indiana 46383
- ³⁸Variable Energy Cyclotron Centre, Kolkata 700064, India
- ³⁹Warsaw University of Technology, Warsaw, Poland
- ⁴⁰University of Washington, Seattle, Washington 98195
- ⁴¹Wayne State University, Detroit, Michigan 48201
- ⁴²Institute of Particle Physics, CCNU (HZNU), Wuhan, 430079 China
- ⁴³Yale University, New Haven, Connecticut 06520
- ⁴⁴University of Zagreb, Zagreb, HR-10002, Croatia

Pion-kaon correlation functions are constructed from central Au+Au data taken at $\sqrt{s_{NN}} = 130$ GeV. The results suggest that pions and kaons are not emitted at the same average space-time point. Space-momentum correlations, i.e. transverse flow, lead to a space-time emission asymmetry of pions and kaons that is consistent with the data. This result provides new independent evidence that the system created at RHIC undergoes a collective transverse expansion.

Two-particle correlations for non-identical particles produced in heavy ion collisions are sensitive to differences in the average emission time and position of the different particle species [1]. Such correlations in data taken at GANIL suggest delayed emission of deuterons with respect to protons [2]. Correlation data from the SPS and AGS also suggest that the pion and proton average space-time emission points do not coincide [2, 3, 4]; a partial explanation is that space-momentum correla-

tions arise from the system's collective expansion [2]. For Au+Au collisions at $\sqrt{s_{NN}} = 130$ GeV, transverse mass spectra, elliptic flow, and deduced pion source radii suggest collective expansion in the transverse plane [5, 6]. Such transverse flow may shift the average emission radii of different particle species by different amounts. Also, different species may kinematically decouple from the system at different times depending upon their interaction cross sections [7]. In addition, the average emission

time for a given species may be delayed significantly if produced dominantly through resonance decay. In this letter, we construct pion-kaon correlation functions from Au+Au data taken at $\sqrt{s_{NN}} = 130$ GeV and investigate whether the pions and kaons are emitted at the same average space-time position. The data was taken by the STAR experiment at the Relativistic Heavy Ion Collider (RHIC) at the Brookhaven National Laboratory.

Non-identical charged particles interact through Coulomb and strong interactions; for the pion-kaon case correlation effects are dominated by the Coulomb interaction. The probability of finding a pair of unlike sign (like sign) particles with small relative momentum in the pair rest frame increases (decreases) depending upon the spatial separation vector \vec{r}^* of the particle freeze-out points in the pair rest frame. To probe this π - K separation, correlation functions $C(k^*)$ are constructed as the ratio of the k^* distribution constructed with particles from the same event (correlated distribution) divided by the k^* distribution constructed with particles from different events (uncorrelated distribution). k^* is the magnitude of the three-momentum of either of the particles in the pair rest frame.

For two particles initially moving towards each other the effects of the Coulomb and strong interactions are different from those for two particles initially moving apart. The technique developed in [1, 2, 8] exploits this difference to study emission asymmetries. Pairs are divided into two groups, which represents either the case where the pions catch up with the kaons or the case where the pions move away from the kaons, depending upon the space-time separation between pion and kaon emission points. Each sample is used to construct two different correlation functions, $C_+(k^*)$ and $C_-(k^*)$, the sign index reflecting the sign of $\vec{v} \cdot \vec{k}_\pi^*$, with \vec{v} the pair velocity and \vec{k}_π^* the pion momentum vector in the pair rest frame. If the average space-time emission points of pions and kaons coincide, both correlation functions are identical. On the other hand, if pions are emitted closer to the center of the source than kaons, pions with larger velocity will tend to catch up with kaons, and the Coulomb correlation strength will be enhanced compared to the case where pions are slower than kaons. Hence, the correlation function C_+ will show a larger deviation from unity than C_- . Pairs can be separated according to the sign of k_{side}^* , k_{long}^* and k_{out}^* , the \vec{k}_π^* projections onto three perpendicular axes in the longitudinally comoving system (LCMS) where the longitudinal component of the pair momentum vanishes [9]. The *out* axis parallels the pair velocity in the LCMS, the *long* axis is the beam axis and the *side* axis is perpendicular to the other two. The corresponding projections of the three-vector \vec{r}^* are r_{out}^* , r_{side}^* , and r_{long}^* . Due to azimuthal symmetry and symmetry over mid-rapidity, $\langle r_{side}^* \rangle = \langle r_{long}^* \rangle = 0$. Thus the ratio C_+/C_- defined with respect to the signs of k_{side}^*

and k_{long}^* must equal unity. On the other hand, if pions and kaons are not emitted at the same average radius in the transverse plane and/or at the same average time, the ratio C_+/C_- defined with respect to the sign of k_{out}^* will deviate from unity, unless these two contributions cancel. Thus, this decomposition allows one to probe specifically the space-time separation between pion and kaon sources in the transverse plane.

Charged particles produced in Au+Au collisions are identified and tracked by the STAR Time Projection Chamber (TPC) [10]. This analysis selects the events with the largest multiplicity of negatively charged particles. These events account for 12% of the most central total hadronic cross section. Selected particles have pseudorapidity $|\eta| < 0.5$. The Au+Au collision point (primary vertex) is required to be within ± 75 cm (along the beam axis) of the TPC mid-plane. The non-correlated pair background is constructed by mixing events whose primary vertices are also separated from each other by less than 10 cm.

Pions and kaons are identified by measuring specific energy loss (dE/dx) in the TPC. When the momentum of pions and kaons exceeds 700 MeV/c, the dE/dx of both species becomes similar which compromises particle identification. In addition, the pion and kaon samples are contaminated by electrons and positrons. The yield of each particle species in the momentum range where the energy losses coincide is interpolated (e^+/e^- contamination) or extrapolated (kaon/pion separation) from the yields measured in the momentum range where there is good separation. In order to quantify the probability of correctly identifying a given species when the dE/dx bands overlap, four probabilities are calculated for each track: the chance that the particle is a π^+ or π^- , K^+ or K^- , p or \bar{p} , or e^+ or e^- [6]. To be accepted as a pion or kaon the probability has to be $> 60\%$. Tracks must point back to within 3 cm of the primary vertex; this removes a large number of secondary pions. Pions must have transverse momentum $80 \text{ MeV}/c < p_T < 250 \text{ MeV}/c$ and rapidity $|y| < 0.5$, while kaons must have $400 \text{ MeV}/c < p_T < 700 \text{ MeV}/c$, and $|y| < 0.5$.

Pion-kaon pair identification probability (product of both particle individual dE/dx probabilities) is required to be larger than 60%. Since the e^+e^- pairs can distort π^-K^+ and π^+K^- correlation functions, the maximum probability allowed for a given pair to be e^+e^- is set at 1%, ensuring negligible contribution. Track pairs that share more than 10% of their TPC space points are discarded in order to avoid track merging errors. Two points are defined as shared if the probability of separating hits produced by them in the TPC is less than 99%. After selecting pion-kaon pairs, the correlation functions are constructed by taking the ratio of the k^* distributions of pairs from the same event to the k^* distributions of pairs from different events.

Primary purity and momentum resolution effects are

taken into account as described below. Primary purity is the percentage of primary pion-kaon pairs in all pion-kaon pairs satisfying all cuts. It is estimated to average 77% for unlike sign pairs and 75% for like sign pairs. The lower limit for each is 54%. This number is the product of two contributions: the probability of identifying both pions and kaons using the dE/dx information and the probability of excluding pions and kaons that do not originate from points close to the collision vertex. Secondary pions which do not contribute to the correlation include decay products of strange hyperons and K_s^0 , and pions produced in the detector material. The fraction of secondary pions is estimated from the K_s^0 , Λ and pion yields in [11, 12, 13]. Detector simulations determine the relative reconstruction efficiency of pions from these different sources. Secondary kaons, being rare, are neglected. Assuming that the non-primary pion-kaon pairs are uncorrelated, the correlation function is corrected as $C_{true}(k^*) = (C_{measured}(k^*) - 1)/purity(k^*) + 1$. The systematic error introduced by this correction is less than 20%.

The effect of momentum resolution depends upon the correlation function shape. Pion-kaon correlation functions are calculated from the pion and kaon momentum and space-time distributions, accounting for both the Coulomb and strong interactions, within the framework developed in [14]. To reproduce the effect of momentum resolution, the correlation function strength is calculated with the true momentum while the correlation function is binned as a function of k^* smeared by momentum resolution. Momentum resolution is estimated at the track level by detector simulations. The space-time distribution is chosen so that the main features of the measured correlation function are reproduced. The correction to be applied to the measured correlation functions is obtained by comparing correlation functions calculated with and without momentum smearing. The correction enhances $C(k^*)$ by 20% (1%) for $k^* < 5$ MeV/c ($5 < k^* < 10$ MeV/c), first and second bins in Figure 1, with a conservative systematic error of $\pm 100\%$ on the correction of these two bins.

The top panels of Figure 1 show the correlation functions for every combination of pion-kaon pairs. The agreement among unlike-sign ($\pi^- - K^+$ and $\pi^+ - K^-$) and between like-sign ($\pi^+ - K^+$ and $\pi^- - K^-$) correlation functions is excellent. The middle and bottom panels show the ratios C_+/C_- for all pion-kaon pair combinations. C_+/C_- with respect to the sign of k_{side}^* and k_{long}^* is unity within statistical errors in accordance with the requirement that $\langle r_{side}^* \rangle = \langle r_{long}^* \rangle = 0$. However, C_+/C_- with respect to the sign of k_{out}^* is significantly larger than unity at small k^* when the interaction is attractive ($\pi^- - K^+$ and $\pi^+ - K^-$) and significantly smaller than unity when the interaction is repulsive ($\pi^+ - K^+$ and $\pi^- - K^-$). These results suggest that pions and kaons are not emitted on

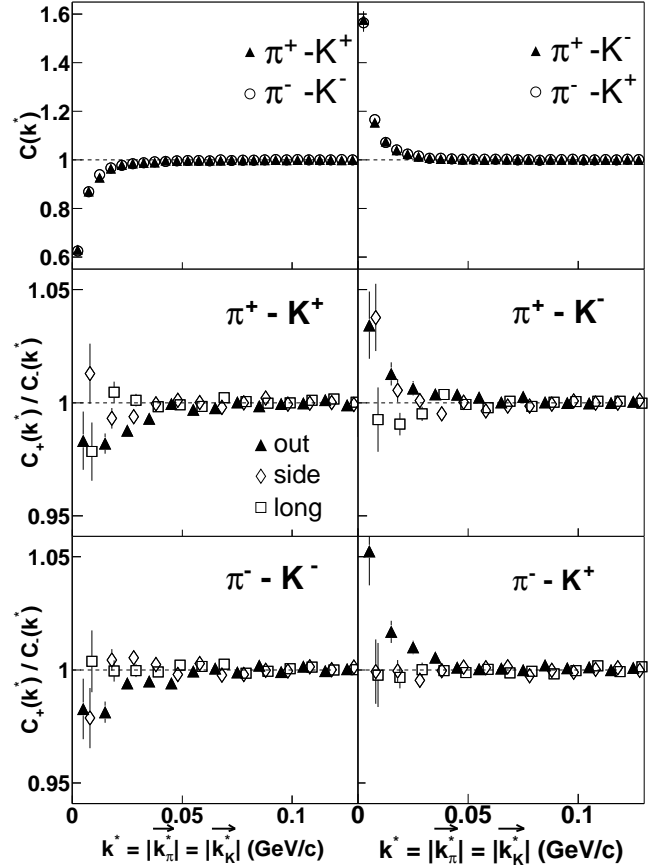


FIG. 1: Top panels: pion-kaon correlation functions $C(k^*)$, the average of $C_+(k^*)$ and $C_-(k^*)$. Middle and bottom panels: ratio of the correlation functions C_+ and C_- defined with the sign of the projections, k_{out}^* , k_{side}^* and k_{long}^* . Errors are statistical only. The horizontal axis of the ratios C_+/C_- for k_{side}^* (k_{long}^*) is shifted by 1 MeV/c (2 MeV/c) to separate the error bars.

average at the same radius and/or time.

In order to understand the measured average space-time shift between pion and kaon sources, we compare the data with the RQMD model and the Blast Wave Parametrization (BWP) described in Ref. [5]. BWP assumes that the system has undergone longitudinal and transverse expansions, and provides the particle space-time and momentum distributions at kinetic freeze-out. The parameters, system outermost radius $R = 13$ fm, freeze-out proper time $\tau = 9$ fm/c, emission duration $\Delta\tau = 0$ fm/c, temperature $T = 110$ MeV, and transverse flow rapidity $\rho(r) = 0.9(r/R)$ (with particle emission radius r) are consistent with parameters obtained by fitting pion, kaon, proton and lambda transverse mass spectra and to pion source radii [5]. The hadronic cascade model, RQMD, also generates transverse flow through rescattering of hadrons [7]. Indeed, turning off hadronic rescattering within this model shuts off transverse flow [15]. In addition, RQMD includes contributions from resonance

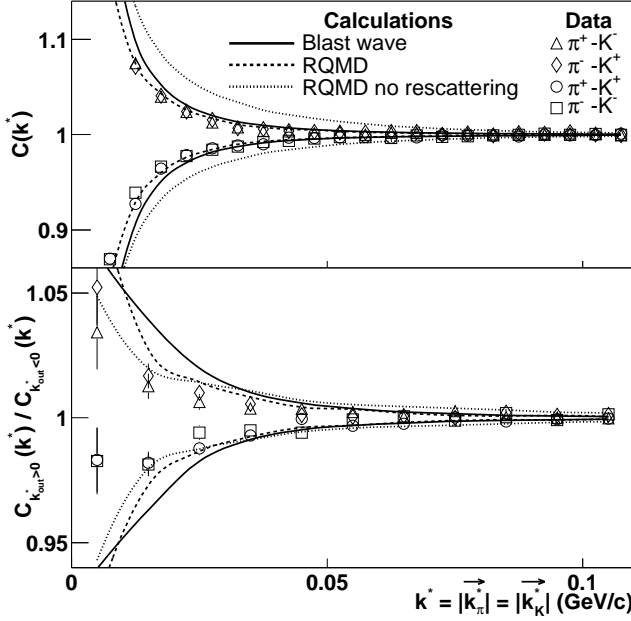


FIG. 2: Comparison of the correlation functions between data and model. Upper panel, $C(k^*)$ correlation function. Lower panel, ratio C_+/C_- with respect to the sign of k_{out}^* .

pair	σ (fm)	$\langle \Delta r_{out}^* \rangle$ (fm)	χ^2 / dof
$\pi^+ - K^+$	12.2 ± 0.6	-6.3 ± 1.2	25.8/26
$\pi^- - K^-$	12.2 ± 0.7	-5.7 ± 1.2	23.6/26
$\pi^+ - K^-$	13.5 ± 0.8	-5.3 ± 1.2	41.9/26
$\pi^- - K^+$	12.7 ± 0.6	-4.6 ± 1.0	43.1/26

TABLE I: Fit results using a three dimensional Gaussian distribution in the pair rest frame. The errors are statistical only.

decay, such as ω , η and ϕ , which shift pion and kaon emission times. RQMD also uses free-particle cross sections for interacting hadrons, but medium effects could alter these interactions differently for pions and kaons.

Figure 2 shows correlation functions $C(k^*)$ and ratios C_+/C_- measured, from BWP, and from RQMD with/without hadronic rescattering. The calculated correlation functions use model space-time and momentum distributions as described in [14], with pion and kaon kinematic cuts chosen to match the data. RQMD and BWP are in qualitative agreement with the measured correlation functions. Turning off rescattering in RQMD leads to a strong correlation, which implies that the pion and kaon sources are too small. On the other hand, RQMD reproduces qualitatively the ratio C_+/C_- with or without rescattering, while BWP overestimates it.

The effect of source size and source shift is disentangled by fitting the correlation functions. In order to insure that the detector acceptance is matched, the particle momenta are taken directly from experimental pion-

	σ (fm)	$\langle \Delta r_{out}^* \rangle$ (fm)	χ^2 / dof
Data	$12.5 \pm 0.4^{+2.2}_{-3}$	$-5.6 \pm 0.6^{+1.9}_{-1.3}$	134.5/110
RQMD	11.8 ± 0.4	-8.0 ± 0.6	205/54
RQMD no rescattering	5.8 ± 0.1	-2.0 ± 0.3	940/54
BWP	9.9 ± 0.1	-6.9 ± 0.3	1020/118

TABLE II: Fit results using a three dimensional Gaussian distribution in the pair rest frame. For the data, the first error is statistical and the second systematic. The errors on the model calculations are calculated by rescaling the χ^2 distribution by the minimum value of χ^2 / dof .

kaon pairs constructed by mixing events that pass all the cuts. The particle positions are set such that the distribution of the relative space-time separation between pions and kaons in the pair rest frame is a three dimensional Gaussian. The free parameters are the Gaussian mean, $\langle \Delta r_{out}^* \rangle = \langle r_{out}^*(\pi) - r_{out}^*(K) \rangle$ ($\langle \Delta r_{side}^* \rangle = \langle \Delta r_{long}^* \rangle = 0$) and the Gaussian width, $\sigma = \sigma_{r_{out}^*} = \sigma_{r_{side}^*} = \sigma_{r_{long}^*}$. The parameters are extracted by fitting simultaneously the correlation functions C_+ and C_- and are summarized in Table 1. Both fit parameters from all four correlation functions are in agreement within statistical errors; combined they give $\sigma = 12.5 \pm 0.4^{+2.2}_{-3}$ fm and $\langle \Delta r_{out}^* \rangle = -5.6 \pm 0.6^{+1.9}_{-1.3}$ fm with a $\chi^2 / \text{dof} = 134.5/110$. Systematic errors are estimated accounting for the discrepancy between the four correlation functions, the dependence on the input momentum distribution, the uncertainties on primary purity and the fit range dependence.

In the Au-Au frame, $\langle \Delta r_{out}^* \rangle = -5.6$ fm in the pair rest frame translates to $\langle r_K - r_\pi \rangle = 3.9$ fm assuming that pions and kaons are emitted at the same time, or $\langle t_\pi - t_K \rangle = 5.4$ fm/c assuming that pions and kaons are emitted at the same average radius.

The parameters σ and $\langle \Delta r_{out}^* \rangle$ may be extracted directly from BWP or RQMD by constructing the $r^* = \sqrt{(r_{out}^*)^2 + (r_{side}^*)^2 + (r_{long}^*)^2}$ and r_{out}^* distributions. However, neither RQMD nor BWP \vec{r}^* distribution is close to a three dimensional Gaussian. Thus, to compare models and data fairly, the correlation functions calculated from RQMD and BWP are fitted in exactly the same way as the data. The extracted fit parameters are compared to the data in Table 2. The large χ^2 / dof values arise because the tails of the \vec{r}^* distributions of RQMD and BWP are not well-described by a three dimensional Gaussian in the pair rest frame. The data appear to be insensitive to these tails due to larger statistical errors.

Consider the qualitative agreement of BWP with the data. At an emission point, the fluid velocity (increases with radius) and the thermal velocity (common freeze-out temperature T for all species in fluid rest frame)

combine to give the observed particle velocity \vec{V} . If the source does not expand, the relative emission probability for given \vec{V} will simply track the fireball spatial density. If the source expands but $T = 0$, particles with \vec{V} will come from the single point where the fluid moves with \vec{V} . At $T \neq 0$ and for constant density and unlimited fireball size, the spread of thermal velocity smears this emission point to a nearly spherical volume whose size increases inversely with particle mass. This volume must be folded with a realistic fireball spatial density distribution, removing contributions from large radial distances. Thus, emission regions for lighter particles remain bigger, but their effective centers are shifted towards smaller radii since a larger fraction of emission region is removed at large r . The measured 2-particle correlation depends upon the projection of these separated volumes onto the outward direction. For our m_t/T (m_t = transverse mass, and $m_t \propto m$ at given V), the relative shift of pions and kaons is small [2] but measurable. There is also an emission time separation: the model has kinetic freeze-out at fixed longitudinal proper time $\tau = \sqrt{t^2 - z^2}$, so the larger size of effective pion source yields emission at later laboratory times t . Thus pions are on average emitted closer to source center and later in time than kaons.

In the RQMD model, transverse flow builds up due to hadronic rescattering. Thus, it is not surprising that the data rule out the RQMD calculation without rescattering ($\langle \Delta r_{out}^* \rangle$ is too small) as there is then no flow to spatially separate pion and kaon sources. However, resonance decays delay the pion average emission time with respect to kaons, which explains why pion and kaon sources appear shifted in RQMD even when rescattering is turned off. Furthermore, such resonance decays increase the apparent size of the source.

To summarize: within the framework of the analyses of pion-kaon correlation functions presented here, the results show that pions and kaons are not emitted at the same average space-time position for Au+Au collisions at $\sqrt{s_{NN}} = 130$ GeV. The data are consistent with BWP and RQMD, i.e. with a system whose dominant feature is a transverse collective expansion. These results significantly challenge models that attempt to explain pion, kaon and proton spectra by purely initial state effects [16, 17]. Furthermore, the application of this non-identical two-particle correlation analysis technique at RHIC offers unique new opportunities to improve our understanding of transverse flow. Such an analysis may also be used to probe at what transverse momentum soft processes (expanding system) give way to hard processes since the space-time emission pattern will substantially change at that momentum.

We wish to thank the RHIC Operations Group and the RHIC Computing Facility at Brookhaven National Laboratory, and the National Energy Research Scientific Computing Center at Lawrence Berkeley National Laboratory

for their support. This work was supported by the Division of Nuclear Physics and the Division of High Energy Physics of the Office of Science of the U.S. Department of Energy, the United States National Science Foundation, the Bundesministerium für Bildung und Forschung of Germany, the Institut National de la Physique Nucleaire et de la Physique des Particules of France, the United Kingdom Engineering and Physical Sciences Research Council, Fundacao de Amparo a Pesquisa do Estado de Sao Paulo, Brazil, the Russian Ministry of Science and Technology, the Ministry of Education of China, the National Natural Science Foundation of China, Stichting voor Fundamenteel Onderzoek der Materie, the Grant Agency of the Czech Republic, Department of Atomic Energy of India, Department of Science and Technology of India, Council of Scientific and Industrial Research of the Government of India, and the Swiss National Science Foundation.

* URL: www.star.bnl.gov

- [1] R. Lednický, V.I. Lyuboshitz, B. Erazmus, D. Nouais, Phys. Lett. B **373** (1996) 30.
- [2] R. Lednický, nucl-th/0305027; Proc. CIPPQG'01, nucl-th/0112011; Proc. XXXII ISMD, nucl-th/0212089.
- [3] R. Ganz *et al.*, Nucl. Phys. A **661** (1999) 448, P. Seyboth *et al.*, Nucl. Phys. B (Proc. Suppl.) **92** (2001) 7.
- [4] D. Miskowiec (E877 collaboration), CRIS'98 proceedings, nucl-ex/9808003.
- [5] B. Tomášik, U. Achim Wiedemann, U. Heinz, Heavy Ion Phys. **17** (2003) 105-143, and F. Retière and M. Lisa, to be submitted to Phys. Rev. C.
- [6] C. Adler *et al.*, Phys. Rev. Lett. **87** (2001) 182301.
- [7] H. W. van Hecke, H. Sorge, and, N. Xu, Phys. Rev. Lett. **81** (1998) 5764.
- [8] S. Voloshin, R. Lednický, S. Panitkin, N. Xu, Phys. Rev. Lett. **79** (1997) 4766.
- [9] R. Lednický, Proc. 8th Int. Workshop on Multiparticle Production, Correlations and Fluctuations (1998) 148, nucl-th/0304063, and, R. Lednický, S. Panitkin, and N. Xu, nucl-th/0304062.
- [10] M. Anderson *et al.*, Nucl. Instrum. Meth. A **499** (2003) 659.
- [11] K. Adcox *et al.*, Phys. Rev. Lett. **88** (2002) 242301.
- [12] C. Adler *et al.*, Submitted to Phys. Lett. B, nucl-ex/0206008.
- [13] C. Adler *et al.*, Phys. Rev. Lett. **89** (2002) 092301.
- [14] R. Lednický and V.L. Lyuboshitz, Yad. Fiz. **35** (1982) 1316 [Sov. J. Nucl. Phys. **35** (1982) 770]. Fortran program provided by R. Lednický.
- [15] C. Adler *et al.* Submitted to Phys. Rev. Lett., nucl-ex/0306029.
- [16] J. Schaffner-Bielich, D. Kharzeev, L. McLerran, R. Venugopalan, Nucl. Phys. A **705** (2002) 494, and nucl-th/0202054.
- [17] H.G. Fischer and the NA49 Collaboration, Nucl. Phys. A **715** (2003) 118.